PCCP

Accepted Manuscript

ROYAL SOCIETY OF CHEMISTRY

www.rsc.org/pccp

Journal Name

ARTICLE

Controllable defluorination of fluorinated graphene and weakening of C-F bonding under the action of nucleophilic dipolar solvent

Received 00th January 20xx,
Accepted 00th January 20xx

DOI: 10.1039/x0xx00000x

www.rsc.org/

Xu Wang [a, b], Weimiao Wang [a], Yang Liu [a], Mengmeng Ren [a], Huining Xiao *[, b], and Xiangyang Liu *[, a]

The effect of solvent on the chemical structure and properties of fluorinated graphene (FG) was particularly investigated in this work. It is found the reduction of FG and the weakening of strong covalent C-F bonding under the action of some dipolar solvents even at room temperature. The rate of the C-F bond rupture reaction is positively influenced by the dipole moment of solvent and fluorine coverage of FG sheets. Meanwhile, the defluorination of FG is controllable through the time and temperature of solvent treatment. These solvents function as the nucleophilic catalysts, promoting the chemical transformation, which leads to a series of change in the structure and properties of FG, such as a decline of fluorine concentration of about 40 % and the reduction of thermal stability and band gap from 3 to 2 eV. After the treatment with dipolar solvent N-Methyl-2-pyrrolidinone, FG maintained a capacity of 255 mAh/g and a power density of 2986 W/kg at a high discharge rate, while the pristine FG could not be discharged at all. This is called the "solvent activation"effect on the electrochemical performance of FG. The finding may draw attention to the effect of various external factors on the chemical structure and properties of FG, which is of great importance for the realization of the FG's potential.

1. Introduction

Fluorinated graphene (FG) is formed by linking the fluorine atom to carbon atoms in graphene.[1, 2] As one of the two-dimensional (2D) derivatives of graphene, it simultaneously inherits important structural and performance features of the graphene and carbon material fluorides (CMFs), exhibiting a great number of remarkable and interesting electronic, optical, thermal, electrocatalytic, magnetic, mechanical, biological, and chemical properties in comparison with its graphene counterparts. [3-7] Furthermore, the strong polarity of the C-F bonds stimulates interesting biological responses, such as promoting the proliferation of mesenchymal stem cells, [7, 8] which captures the attention of scientists in the field of biology. These properties of FG can be tailored for different needs by altering the concentration of fluorine and the nature of C-F bonding, and the later factoris being given new importance in recent years. For example, Sun et al. reports that semi-ionic C–F bonds show a high discharge voltage and an excellent rate capability, being superior to covalent C-F bonds. [9] Lee et al. introduced the ionic C-F bond to graphene which can be selectively reduced and recovers its conductivity. [10] Moreover, graphene can berolled into 1D nanotubes or stacked into 3D graphite. [11] For the same reason, the 2D fluorogaphene can be considered as a basic building block for the CMFs of all other dimensionalities such as graphite fluoride, fluorinated carbon nano-tube and fluorinated fullerene. Studying the relationship between the chemical structures and properties of FG is favourable to accurately understand and utilize that of other CMFs.

It is commonly accepted that the covalent C-F bond has the high bond dissociation energy (BDE, about 460 kJ/mol) and possesses the excellent stability. [12] The highly fluorinated FG, which is mainly composed with covalent C-F bonds, is commonly considered to have good chemical stability and thermal tolerance. [2, 13-15] To maximize their potentials, the stability of FGs in environmental should be thoroughly evaluated. It is inevitable for the FG sheets to have contact with various kinds of solvents during application and storage, especially when they are used as the cathode material for lithium batteries, [16-19] as raw materials for preparing functionalized carbon materials, [20-22] or as

a. State Key Laboratory of Polymer Materials Engineering, College of Polymer Science and Engineering, Sichuan University, Chengdu, Sichuan, 610065, P.R. China. E-mail: lxy6912@sina.com; Fax: +86 28 85405138; Tel: +86 28 85403948

b. Department of Chemical Engineering, University of New Brunswick, Fredericton, NB $E_3B\ 5A_3$, Canada. E-mail: hxiao@unb.ca

† Electronic Supplementary Information (ESI) available: Synthesis of the spongy graphene oxide; SEM images of reduced spongy graphene oxide (RSGO);XRD spectra of FG samples disposed by different solvents: FG, Chloroform-FG, Ethanol-FG, Methanol-FG, DMF-FG, DMAc-FG and NMP-FG (top to bottom);XPS F 1s spectrum of FG and samples treated by solvent. See DOI: 10.1039/x0xx00000x

nanofiller for producing advanced composite materials.[23] However, few of studies on the FG's sensitivity to solvents are currently available.

In this study, we found that the interesting transformation in terms of chemical structure of FG took place in some dipolar solvents even at room temperature. Thus, the effect of solvents on the chemical structure and properties of FG was explored by X-ray diffraction (XRD), X-ray photoelectron spectroscopy (XPS), fourier transform infrared spectroscopy (FTIR), thermogravimetric analysis (TGA), transmission electron microscope (TEM), UV-vis diffuse reflectance spectroscopy etc.. The effect of solvent on the chemical structure of FG is confirmed, which results in the controllable reduction of FG and the weakening of strong covalent C-F bonding. As a result, the electrochemical performance of FG is significantly improved, but its thermostability decreases simultaneously. It is evident that the choosing of solvent is important for the performance of FG in various research and application fields. Overall, the finding will draw more attention to the bond weakening effect of various kinds of external influencing factors on the physical and chemical characterizations of FG.

2. Experimental

2.1 Synthesis of FG

The FG was prepared according to the method reported in reference 23. [23] Spongy graphene oxide (GO) (100 mg) was placed in a Petri dish set in a vacuum desiccator, where a piece of filter paper saturated with the chemical reducing agent hydrazine (80 wt %water solution, 5 mL) was placed in the desiccator for the reduction. The synthesis of the spongy graphene oxide is shown in Supporting Information in detail. The reducing reaction time is 72 h and this sample was called as reduced spongy graphene oxide (RSGO). Its detail structure is shown in Figure S2. Fluorination was carried out in a closed stainless steel (SUS316) chamber (10 L) equipped with a vacuum line. 100 mg RSGO was put in the chamber. After exchanging nitrogen three times, we removed the residual oxygen and moisture in the chamber. 50 KPa F_2/N_2 mixed gas was introduced in to the chamber at room temperature. Fluorination occurred when the temperature was increased from room temperature to 210 ^{o}C at a rate of 4 ^{o}C/min, and was held steady at this temperature for 180 min. Residual F_2 and by-products in the chamber were removed at once by vacuum and absorbed by an alkali aqueous solution. Then, the fluorinated samples were taken out and preserved in dry atmosphere.

2.2 Solvent treatment

A certain amount of FG (approximately 20 mg) was ultrasonic-dispersed (280 W) into one kind of solvent (50 mL) among chloroform, ethanol, methanol, dimethyl formamide (DMF), dimethylacetamide (DMAc) and NMP with ultrasonic treatment (280 W) for 5 min. After standing for different time, the dispersion solutions were filtered by a polytetrafluoroethylene microporous membrane (0.22 μm). The FG papers were obtained and dried in a vacuum oven at 60 °C for 24 h.

2.3 Characterizations

Wide angel X-ray diffraction (WXRD) was carried out on a Philips X'Pert PRO-MPD instrument. The surface chemical composition of fluorinated and non-fluorinated samples was examined by XPS with monochromatized Al Ka rays (1486.6 eV) under the circumstance of 12 kV×15 mA, Kratos, Inc., at RT and at 2×10^{-7} Pa. Binding energies were referenced to the hydrocarbon peak at 284.8 eV. The take-off angle was 20ºwith sampling depths of approximately 6~10 nm. FTIR was recorded by a Nicolet 560 Fourier transform spectrometer. TEM was performed on Tecnai G2 F20 S-TWIN. TGA was performed on Netzsch 209 TG instruments. UV-vis diffuse reflectance spectroscopy measurements were performed on a UV-VIS spectrophotometer of Shimadzu UV2100.

For electrochemical tests, FG electrodes were assembled with FG (about 75% by weight, w/w) and acetylene black (15%, w/w) to ensure the electronic conductivity in the presence of polyvinylidene difluoride (PVDF, 10%, w/w) as a binder. Dibutylphtalate was then added until the mixture becomes homogeneous and slightly viscous. The mixture was then poured on an aluminum foil and allowed to dry in a vacuum oven at 80 °C for 24 h. Cathode discs were cut from the film, about 1.2 cm in diameter, which contain about 2.0 mg FG sample. Coin cells were assembled in a dry box filled with argon and was made of a metallic lithium disc for the anode, a microporous polypropylene separator soaked with a 1 molar solution of $LiBF_4$ in propylene carbonate (PC) : 2-dimethoxy ethane (DME) (1:1 w/w.) electrolyte and the FG based cathode. The coin cells were discharged at different rates at room temperature.

3. Results and discussion

3.1 effect of solvent on the properties of FG

FG with a high fluorine/carbon ratio (F/C ≈1.0) was synthesized from spongy graphene by direct fluorination using fluorine gas as a fluorinating agent. After fluorination, the alveolate structure is retained (Figure 1b). The color of sample changes from black to white with the introduction of fluorine atoms (Figure 1a). The FG sample is denoted with FG. Figure 1c and 1d show the exfoliated FG sheets in chloroform by ultrasonic. According to our previous reports,[23] the yield of monolayered FG is about 10 % and the number of layers is mainly in the range of 2~5. The broad solvent dispersibility of FG has been reported by Gong and Zhu et al.. [24, 25] Here, six kinds of solvent were chosen: chloroform, methanol, ethanol, dimethylformamide (DMF), dimethylacetamide (DMAc) and N-methyl-pyrrolidone (NMP), which are widely used for the dispersion of FG, graphene oxide and other graphene derivatives. [26, 27] The dispersibility and stability of FG in these solvents were tested as shown in Figure 1e.

Journal Name

ARTICLE

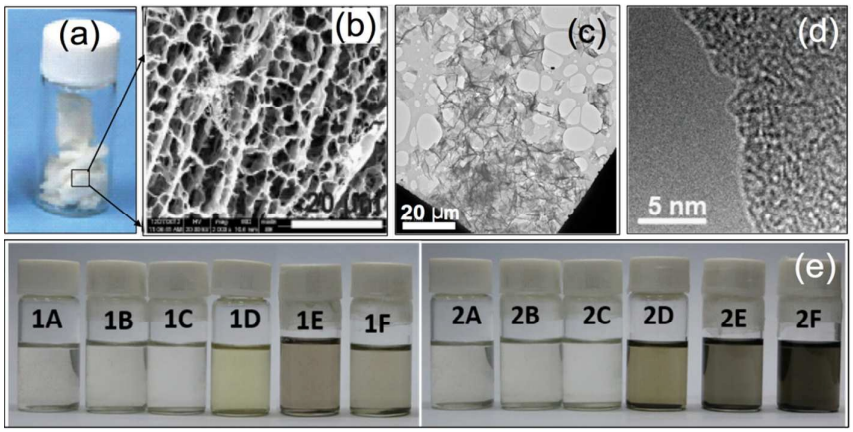

Figure 1. (a) photographs and (b) SEM picture of fluorinated graphene; (c) TEM and (d) HRTEM micrographs of the FG sheets; (e) Optical pictures of the fluorographene suspension (0.1 mg/mL) of chloroform (1A, 2A), methanol (1B, 2B), ethanol (1C, 2C), DMF (1D, 2D), DMAc (1E, 2E) and NMP (1F, 2F). Left: dispersion without standing after sonication and slight shaking. Right: dispersions standing for 12 h after sonication.

FG is dispersed in one solvent for a certain amount of time and then filtered out for structural analysis and property testing. The resulting materials are respectively denoted with chloroform-FG, ethanol-FG, methanol-FG, DMF-FG, DMAc-FG and NMP-FG. As shown in Figure 1, the FG dispersion of chloroform, methanol and ethanol are almost colorless due to the high light transmission of FG, and the corresponding FG papers are light gray as the inset pictures shown in Figure 2. In contrast, the colors of DMF, DMAc and NMP solutions are deeper, seeming that the FG sheets have been reduced in these solvent, while the FG papers are also dark such as the NMP-FG paper shown in the inset pictures of Figure 2.

The darkening of color visually indicates that the band gap of FG is reduced. In order to obtain the value of the band gap, the absorbance of the FG papers in UV-vis region was measured by UV-vis diffuse reflectance spectroscopy. FG papers from the chloroform, methanol and ethanol solutions were found to have no light absorbance at visible frequencies and to start absorbing light only in the blue range (Figure 2), proving that the FGs are a wide-gap semiconductor with Eg ≥3.0 eV which is consistent with the value of FG reported in previous literature. [4, 28] In comparison, the papers from DMF, DMAc and NMP solutions show a lower band gap, about 2.0 eV, due to the increase of the light absorbance at visible frequencies. This provides a feasible method for the adjusting of the band gap by the dispersing of FG sheets in different solvents for different time durations.

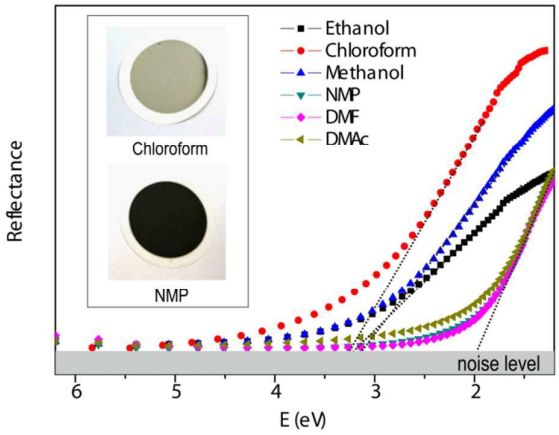

Figure 2. Reflectance result of FG paper. The inset pictures are the FG paper from the chloroform and NMP solution.

Figure 3 and 4 shows TGA lines of FG samples disposed by different solvents for different times and the corresponding differential thermal analysis (DTA) data. The mass loss of pristine FG mainly occurs at around 545 °C. After solvent treatment, chloroform-FG, ethanol-FG and methanol-FG retain excellent thermal stability, while the thermal stability of NMP-FG, DMF-FG and DMAc-FG decreases significantly with mass loss mainly occurring below 400 °C. Decomposition at such a low temperature indicated that the resulting C-F bonds are non-covalent bonds. After solvent treatment for 1 hour, the mass loss peaks are mainly at the low temperature zone (below 400 °C) while there are still obvious peaks at the high temperature zone

(400 ~ 600 °C) due to the residues of C-F covalent bonds. 24 hour later, the mass loss peaks at the high temperature zone disappeared, reflecting that the chemical transformation is completely achieved. The decomposition peaks at the low temperature zone are some irregular shapes due to the existence of a small amount of solvent residue and some oxygenated groups. In addition, the thermal decomposition behavior of FGs treated by solvent is noticeable different with that of FGs with same F-content directly prepared by fluorination without solvent treatment reported in reference 23. Overall, some solvents will exercise a profound influence upon the final thermal properties of FG after solvent treatment, which must be taken into consideration when the high thermal stability of FG is required. What is more, the decrease of thermal stability also reflected a high reactive potential which indicated the great impact of this solvent upon the electrochemical performance of FG.

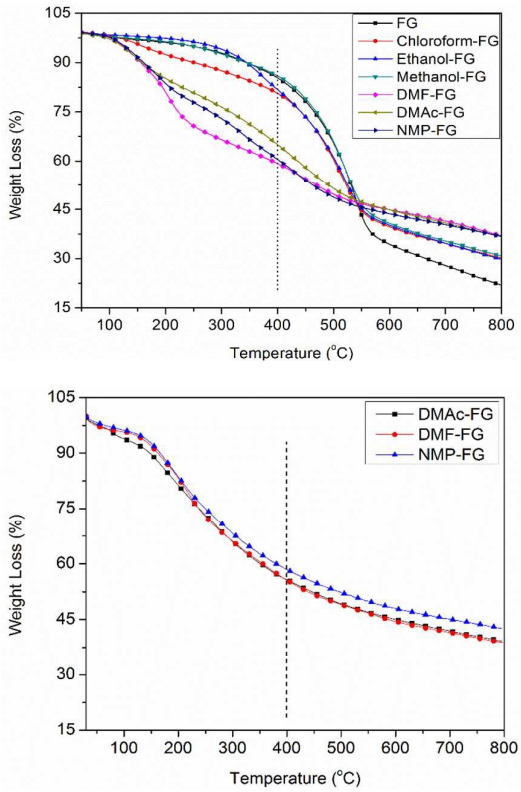

Figure 3. TGA lines of FG samples disposed by different solvents for different times (1 hour or 1 day) at heating rate of 10 °C/min under N_2 atmosphere: after 1 hour (top), after 1 day (bottom).

Figure 5 shows the galvanostatic discharge curves of FG samples, pristine FG and NMP-FG. At a rate of 25 mA/g, the specific capacities for FG and NMP-FG are 706 mAh/g and 603 mAh/g, respectively. The F/C ratio of NMP-FG is significantly lower than that of the starting FG, but their specific capacities at low rate is similar. Meanwhile, NMP-FG demonstrates a superior rate capability in comparison with FG. For example, a high capacity of 255 mAh/g is still obtainable for NMP-FG at the rate of 1500 mA/g, while FG cannot be discharged at all. This indicates the higher reactivity of the C-F bonds in NMP-FG, which is able to provide enough electrons for maintaining a larger discharge rate. Table 1 summarized the discharge rata, the specific capacity, the energy density and the power density. Electrochemical behaviour strongly depends on the composition of the fluorinated compounds and their reactivity with the electrolyte. The values of the energy and power densities of NMP-FG are obviously larger than that of FG, especially at the higher discharge rata. This reminds the scientists that the effect of solvent on chemical structure of fluorinated compounds could not be ignored in the process of pursuing the outstanding cathode materials with high energy and power density.

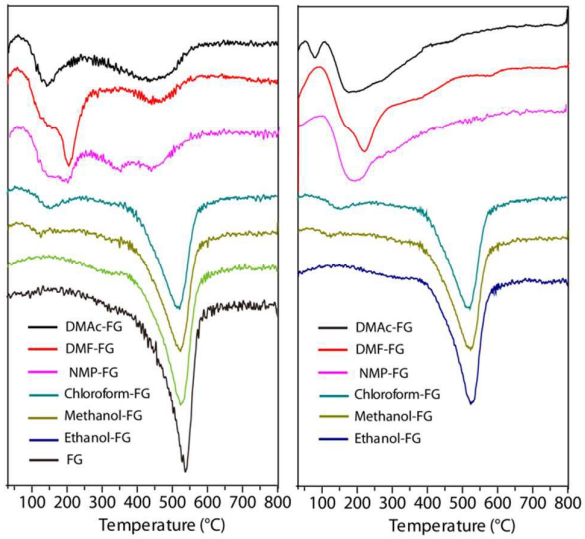

Figure 4. DTA data of FG samples disposed by different solvents for different times (1 hour or 1 day) at heating rate of 10 °C/min under N_2 atmosphere; after 1 hour (left): DMAc-FG, DMF-FG, NMP-FG, Chloroform-FG, Ethanol-FG, Methanol-FG and FG (top to bottom); after 1 day (right): DMAc-FG, DMF-FG, NMP-FG, Chloroform-FG, Ethanol-FG and Methanol-FG (top to bottom).

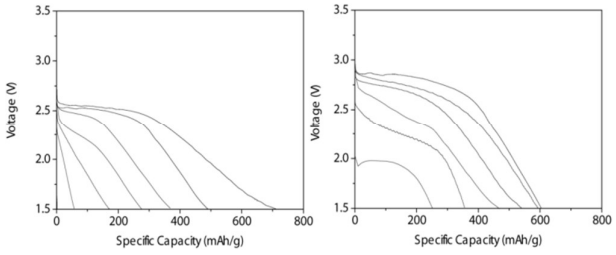

Figure 5. Discharge profile of Li/FG cells at different rates: the galvanostatic discharge curves of FG (left) and NMP-FG (right) at a rate of 25, 50, 100, 500, 1000, and 1500 mA/g, respectively (top to bottom).

Journal Name

ARTICLE

Talbe 1. The specific capacity, the energy density and the power density of FG (left) and NMP-FG (right) at different discharge rata

	Discharge rata (mA/g)	25	50	100	500	1000	1500
FG	Specific capacity (mAh/g)	706	493	332	274	167	56
	Energy density (W/kg)	1289	945	623	455	313	94
	Power density (W/kg)	65	124	245	1125	--	--
NMP-FG	specific capacity (mAh/g)	603	596	521	466	354	255
	Energy density (W/kg)	1397	1244	1103	765	682	423
	Power density (W/kg)	73	141	277	1342	2219	2986

Figure 6 show transmission electron microscopy (TEM) images of the Chloroform-FG and NMP-FG sheets. Selected area electron diffraction (SAED) was performed along the [001] zone axis. The diffraction pattern of the NMP-FG sheets depicted in Figure 6d showed a crystalline structure. The first ring came from the (1100) reflection recovered the hexagonal symmetry of the [0001] diffraction pattern, indicating the reformation of the aromatic region. [29] The NMP-FG sheets with more than six bright hexagonal spots contain the fluorinated and reduced regions simultaneously. [30] The reduced regions with higher conductivity are suitable for the electron transmission, which offers less internal resistance and thus higher electrochemical performance.

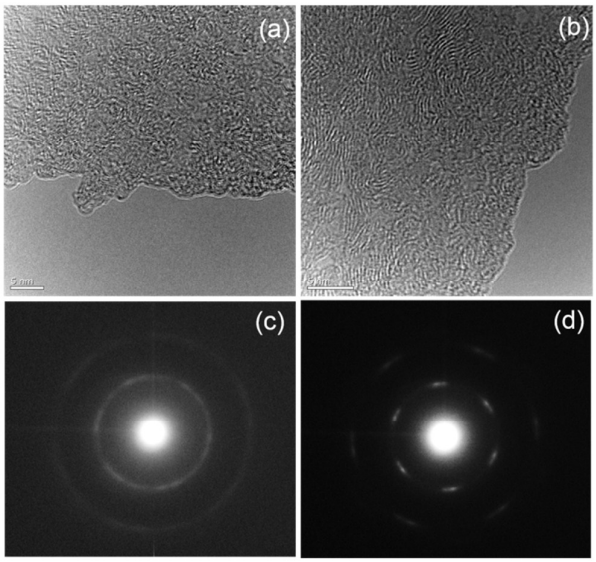

Figure 6. HRTEM micrographs and (c) Selected area electron diffraction pattern of Chloroform-FG (a and c) and NMP-FG (b and d)

Meanwhile, XRD spectra data are shown in Table 2 and Figure S3. Interlayer spacing d(001) is 7.21,7.04 , 7.47 and 7.22Å, respectively, for pristine FG, chloroform-FG, ethanol-FG and methanol-FG. Compared with pristine FG, the position of peak due to the (001) diffraction does not have an obvious shift for FGs treated with chloroform, methanol and ethanol, still being at around 2θ= 12.49°. However, under the action of DMF, DMAc or NMP, the peak is shifted to a lower angle, 2θ≈9.60°. The corresponding d(001) is 9.45, 9.60 and 9.56, respectively. The interlayer spacing of the fluorinated graphene paper from around 7.2 Å increased to 9.5 Å. the increase of interlayer spacing also plays as an important role in achieving the excellent discharging property. These weakened C-F bond shows a larger bonding length in comparison with the starting covalent C-F bond, which increases the inter-layer spacer and thus promotes the diffusion of solvated Li^+ ions. It is confirmed that the solvent effect of DMF, DMAc, and NMP results in the increasing of interlayer spacing and thus promotes the diffusion of Li^+ ions.

Expect the elongation of C-F bonds, the reasons for increasing of interlayer spacing may exclude the ultrasonic exfoliation of FG sheets in different solvents. The particle size analysis by dynamic light scattering is used to reveal the difference of the exfoliation degree, It has a large errors for the precise sizes of graphene sheets, but would show the obvious tendency of solvent effect. The average particle size of NMP-FG is about 1.9 µm while that of Chloroform-FG is 6.2µm. The smaller size corresponds to the larger special surface area which facilitates improving the electrochemical performance of cathode materials.

This solvent effect on electrochemical performance of FG sheets here in can be called “solvent activation” which should be given a great attention with the search for the cathode material of high energy and high power densities lithium batteries.

3.2 Chemical structure of FGs before and after solvent treatment

The higher electrochemical performance of the treated FGand the lower thermostability reflected the weakening effect of solvent on the C-F bond of FG.In order to identify the exact cause, the chemical structures of the FGs before and after solvent treatment were investigated with FTIR, Raman and XPS. The FTIR spectra are shown in Figure 7.

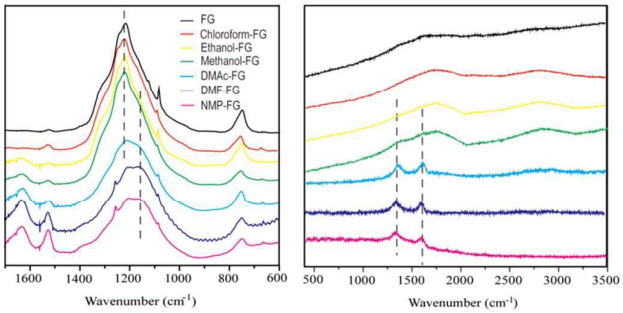

Figure 7. FTIR spectra (left) of FG samples dispersed in different solvents: FG, Chloroform-FG, Ethanol-FG, Methanol-FG, DMAc-FG, DMF-FG, and NMP-FG (top to bottom); Raman spectra (right) of FG samples dispersed in different solvents: FG, Chloroform-FG, Ethanol-FG, Methanol-FG, DMAc-FG, DMF-FG, and NMP-FG (top to bottom).

The absorption band at around 1200 cm^{-1} is assigned to the stretching vibration of the C-F bond ($v_{(C-F)}$) in carbon material fluorides (CMF), and the special peak position shifts with the changing of C-F bonding. In this study, the peak position of pristine FG is at 1221 cm^{-1}, which is attributed to the stretching vibration of covalent C-F bonds. The peak shape, intensity and position of$v_{(C-F)}$ in the FTIR spectra of Chloroform-FG, Ethanol-FG and Methanol-FG have no change in comparison with that of pristine FG, demonstrating that the nature and number of C-F bonds remain the same. By contrast, the $v_{(C-F)}$ absorption bands in the spectra of NMP-FG, DMF-FG and DMAc-FG are obviously changed. The peak position shifts to the lower wave number, from 1221 to 1150 cm^{-1}. Raman spectra are shown in Figure 7. One 533 nm He-Ne laser was chosen as the exciting laser and the testing range was 400-3500cm^{-1}. The typical features of graphene almost disappeared completely in the spectrum of FG due to the high fluorination degree. After being treated by DMAc, DMF, and NMP, the D and G bands reappear in the corresponding Raman spectra. This result reveals the partial reduction of FG sheets in these three solvents, being consistent with that of FTIR analysis.

The XPS data in table 2 show that the value of F/C ratio of FG, chloroform-FG, ethanol-FG, methanol-FG, DMF-FG, DMAc-FG, and NMP-FG respectively is 0.96, 0.93, 0.91, 0.91, 0.64, 0.65, and 0.58. Corresponding C1s peaks of XPS spectra were also investigated in Figure 8, and assignments are listed in Table 3. The existence of peak (1) at about 285 eV (assigned to the bare carbon atoms) in the spectrum of FG reflects that the starting FG is close but not stoichiometric, even though the value of F/C ratio is about 1. For DMF-FG, DMAc-FG, and NMP-FG, the peak of 285 eV increased obviously while the peaks at around 289 eV decreased, which proves the reduction of FG in its dispersion of DMF, DMAc, and NMP.The reductions of F-content for NMP-FG, DMF-FG and DMAc-FG are evident as shown in table 1, among which the value of NMP-FG is the lowest. Meanwhile, colors of the DMF-FG and DMAc-FG dispersions are similar while that of NMP-FG is deeper in Figure 1e. In conjunction of these two results, it seems that the extent of the chemical transformation in NMP is higher than that in DMF and DMAc.

Table 2. XPS data of elements content and XRD data of interlayer spacing for the FG samples disposed by different solvents for 24 h

Samples	XPS data of elements content					chemical formal	XRD data
	C (at %) ±0.5	F (at %) ±0.5	O (at %) ±0.5	C1s of C-F (eV)	F1s of C-F (eV)	$C_1F_XO_Y$	d(001) (Å) ±0.3
FG	47.7	45.7	6.6	290.1	689.2	$C_1F_{0.96}O_{0.14}$	7.21
Chloroform-FG	48.4	44.8	6.8	289.8	689.2	$C_1F_{0.93}O_{0.14}$	7.04
Ethanol-FG	48.8	44.5	6.7	289.6	689.1	$C_1F_{0.91}O_{0.14}$	7.47
Methanol-FG	48.8	44.4	6.8	289.6	689.1	$C_1F_{0.91}O_{0.14}$	7.22
DMF-FG	56.3	35.9	8.2	288.7	688.0	$C_1F_{0.64}O_{0.15}$	9.45
DMAc-FG	56.5	35.6	7.9	288.6	688.0	$C_1F_{0.63}O_{0.14}$	9.60
NMP-FG	57.5	33.6	8.9	288.3	687.9	$C_1F_{0.58}O_{0.15}$	9.57

Journal Name

ARTICLE

The C 1s curve fit spectrum of fluorinated samples exhibits three components corresponding to fluorine related groups, peak (3) at about 289 eV, peak (4) at about 291 eV and peak (5) at 292 eV, which are assigned to CF_1, CF_2, and CF_3, respectively (in Figure 8). The CF_2, and CF_3 groups are formed at the edge or the new defects of FG sheet. The C 1s binding energy peak position of the CF_1 group of NMP-FG, DMF-FG and DMAc-FG decreased to 288.7 eV from around 289.5 eV, compared to that of pristine FG, chloroform-FG, ethanol-FG and methanol-FG. F 1s binding energy of the C-F bonds shifted to a lower energy from 688.5 to 687.9 eV as shown in Figure S4. The decreasing of binding energy, combining with the FTIR results, confirm the weakening effect of solvents NMP, DMAc and DMF on the C-F bonds.

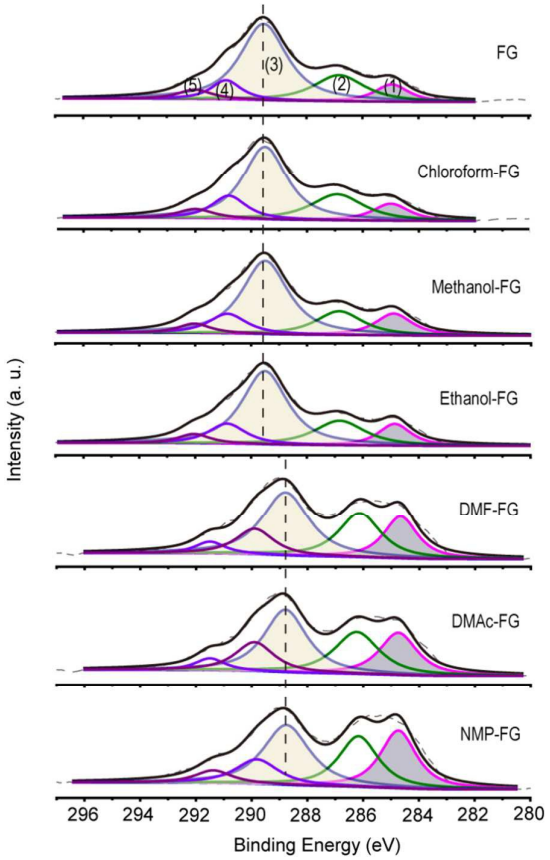

Figure 8. Curve-fitting of XPS C 1s spectrum of of FG samples dispersed in different solvents: FG, Chloroform-FG, Ethanol-FG, Methanol-FG, DMF-FG, DMAc-FG and NMP-FG (top to bottom).

The C-F bonds show a different character due to the difference of fluorination route and starting carbon materials, which plays an important role in determining the performance of the final CMFs in many areas. In order to differentiate them, the "covalent" versus the "semi-ionic" binding state for C-F bonds has been proposed for graphite [31] and carbon nanotubes [32] and extended to grapheme [33] based largely on the positions of the F 1s peak in XPS data and the IR absorption band ascribed to the C–F stretching mode. Sun et al. reports that semi-ionic C–F bonds show a high discharge voltage and an excellent rate capability, being superior to covalent C-F bonds; [9] Lee et al. introduced the "semi-ionic" C-F bond to graphene which can be selectively reduced and recovers its conductivity; [10] and, it is accepted that the covalent C-F bond has a high bond dissociation energy (BDE, about 460 kJ/mol) and possesses the excellent stability compared to the semi-ionic C-F bond. [12] However, this interpretation has been called into question by Sato et al. [34] according to the X-ray diffraction data which does not show the presence of any such "semi-ionic"bond. This group attributed the variations of F peak positions in XPS to differences in the local degree of fluorination. The view is supported by Stine et al.. They considered that the C-F bonds are all covalent in the fluorinated carbon materials while the nonvolatile vs the volatile fluorination sites are likely the result of differing electron density within the C-F bonds due to the local changes in fluorine content. [35] Meanwhile, Bettinger et al. [36] and Asanov et al. [37] confirmed that one IR absorption peak of F-C bond at a lower wavenumber (~1100 cm^{-1}) was assigned to the vibrations in a C-F bond surrounded by bare carbon atoms, namely lower density of fluorine coverage.

Applying the observations of above several groups to our own system gives us an approximate explanation of the observed FTIR and XPS. It is inevitably that the solvent treatment changed the chemical environment of C-F group in the graphene sheets. After being dispersed in some dipolar solvent, there are more isolated C-F bonds surrounded by bare carbon atoms in the FG sheets due to the lower fluorine content, which results in the lower electron density within the C-F bonds because of the hyperconjugation. This results in the decreasing of the C-F binding energy.

It is inevitable that the chemical and physical properties of FG will change dramatically with the weakening of its covalent C-F bonds. The weakened C-F bonding is relatively unstable and highly reactively. The drastic reduction of thermal stability and significant improvement of electrochemical performance of FG after solvent treatment definitely confirm the transformation of bonding nature.

3.3 Mechanism and factors of the solvent effect

Several groups have successfully proved the broad solvent dispersibility of fluorinated graphene. Fredorov et al. [38] found that the dispersions of fluorinated graphene formed in polar organic solvents, such as *tert*-butanol, 2-propanol, ethanol, and

methanol, capable of establishing hydrogen bonds -F···H-. Gong et al. [24] reported that FG also favors the solvents having the free P_z orbital, such as NMP, phenylethylene (PS), dimethyl sulfoxide (DMSO), and tetrahydrofuran (THF), which can behave as an electron acceptor and forms pseuda-hydrogen bond with FG's (C_nF)-F groups. Ren found ultraviolet irradiation can reduce fluorinated graphene with assistance of some aromatic solvents. [39] The high reactivity of fluorinated graphene with nucleophile has been reported.[40, 41] However, the reduction effect of solvent on FG has not been noticed. Even there was a decrease of fluorine content during sonic exfoliation, it is attributed to the action of ultra-sonic treatment.

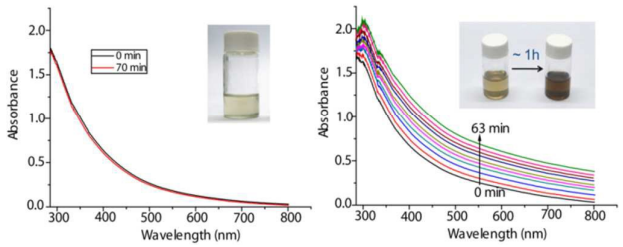

Figure 9. Change of the UV-vis spectra of the FG dispersion in ethanol (left) and NMP (right) through bath ultrasonication (only 30 second)

Figure 9 shows how the UV-vis absorption spectrum of FG in ethanol and NMP respectively changes over time. It can be seen that the spectrum of the ethanol solution does not have an obvious change after 70 min. The NMP solution exhibits enhanced absorption in the whole wave number range even without the assistant of external factors (such as heat, light, or sonic treatment), and its color changes rapidly. This visually reflects the chemical structure of FG sheets dispersed in NMP changes significantly and fast without sonic treatment. That is, the change of the chemical structure and properties of FG is exactly due to the action of solvent.

Table 4. Data of dipole moment and dielectric constant of solvents

Solvent	dipole moment ($\mu/10^{-30}$ C·m)	dielectric constant
chloroform	3.83	5.1
methanol	5.67	32.7
ethanol	5.63	24.5
DMF	12.73	36.7
DMAc	12.41	37.8
NMP	13.64	32.2

Lee et al. reported the reduction of FG under the action of acetone, but it was supposed that only the ionic C-F bond was broken as $2C_2F$ (semi-ionic) + $CH_3C(O)CH_3$(l) →HF + 2C(s) + C_2F (covalent) + $CH_3C(O)CH_2$(l), while the covalent C-F bond is stable in the dispersion of acetone. [10] Different to their conclusion, the strong covalent C-F bonds are proved to be unstable in some solvents such as NMP, DMAc, and DMF in our study. Some covalent C-F bonds were eliminated in the dispersions of these solvents, which results in that the residual covalent C-F bonds were weakened due to the change of chemical environment.

If the dipole moment and dielectric constant is respectively greater than 8.34 $\mu/10^{-30}$ C·m and 15, the solvent is called "dipolar solvent". Due to its nucleophilicity, the dipolar solvent facilitates the sn2 reaction though interaction with the electron deficient atoms. As shown in Table 4, the dipole moment of NMP, DMF and DMAc is respectively 13.64, 12.73 and 12.41 $\mu/10^{-30}$ C·m, higher than 8.34 $\mu/10^{-30}$ C·m, and dielectric constant is respectively 32.2, 36.7, and 37.8, which demonstrates that they all are dipolar solvents. Dipolar solvents can interact via dipolar-dipolar interaction with the electron-deficient carbon atom of C-F bond, which can provide the energy released from the dipolar-dipolar interaction. The High polar solvent has strong solvability and consequently can release a large amount of energy. Here, the solvent molecules function as the nucleophilic catalysts, promoting the rupture of partial C-F bonds which is similar to the unimolecular heterolysis of halides, and the carbon atom of covalent C-F bond is more likely to be attacked by solvent molecule due to it electron-deficiency. Chloroform, methanol and ethanol interact with the fluorine atom of C-F bond by establishing hydrogen bonding according to the previous reports, which seems not to promote the rupture of C-F bonds. The reduction of FG proceeds easily in the dispersions of dipolar solvents with high dipole moment and dielectric constant. From the above results, the chemical structure of FG transformed fastest in the solvent NMP with the highest dipole moments. Due to its high polarity, the nitrogen atom of NMP molecule atom has a high electron density, showing the high nucleophilicity. It is indicated that the rate of transformation of C-F bonding nature increases with the nucleophilicity of solvent.

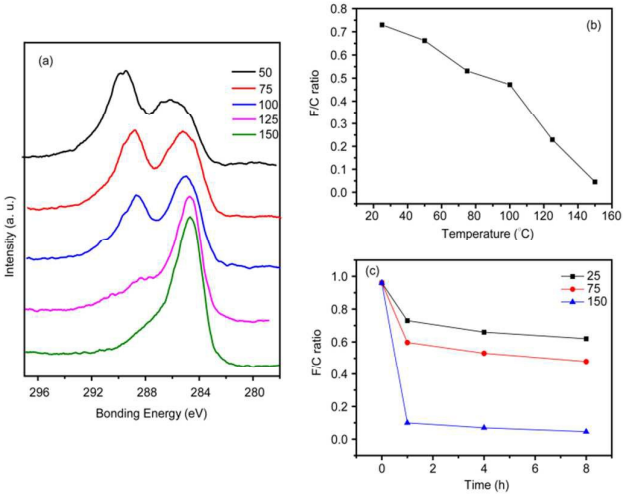

Figure 10. Defluorination effect of NMP on fluorinated graphene with different treatment temperature and time. a) C 1s XPS spectra of FG samples treated by NMP at different temperature for 1 hour (top to bottom: 50 °C, 75 °C, 100 °C, 125 °C, 150 °C); b) F/C ratio values of FG sample in NMP as a function of temperature based on the XPS data; c)

F/C ratio values of FG sample in NMP as a function of time at 25 °C (square), 75 °C (circular), and 150 °C (triangle).

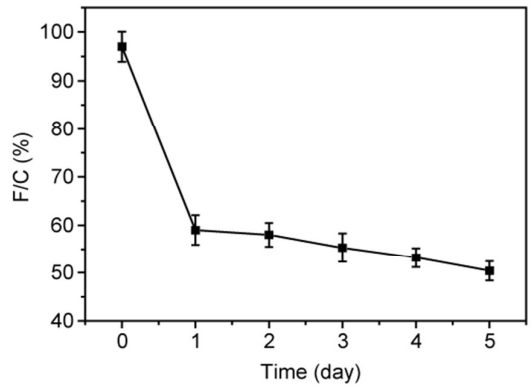

Figure 11. F/C ratio values of FG sample in NMP as a function of time.

NMP was used to study the effect of the solvent treatment conditions on the CxFy composition in this work. Defluorination effect of NMP on fluorinated graphene with different treatment temperature and time was shown in Figure 10. As shown in Figure 10a, the intensity of peak in C1s spectra at around 289 eV, which is assigned to the carbon atom of C-F, decreased significantly with temperature, while the peak of non fluorinated carbon atoms at around 285 eV is correspondingly enhanced. This results in the obvious decrease of F/C ratio with temperature in Figure 10b. For FG sample treated at 150 °C, the value has been as low as 0.05. Figure 10c and Figure 11 shows the F/C ratio values of FG sample in NMP as a function of time. Similar to temperature, the extension of time reduces the F/C ratio value of the treated FG sample, especially in the first one hour. It is supposed that the reduction of fluorinated graphene generated fluorine radicals. The eliminated fluorine would in-situ react with the solvent molecules and product HF and fluorinated solvent molecules. However, the structure of fluorinated products was complex and uncertain due to the high reactivity and low selectivity of fluorine radicals.

As shown in Figure 11, the treated FG lost roughly 40% of the initial fluorine coverage after 5 days of dispersion. The most of the loss occurred in the first 1 day. In the following 4 days, the rate of reaction decreases significantly, even though the residual C-F bonds have been weakened. This is supposed to be due to the rapid decrease of fluorine coverage and the corresponding steric repulsion among C-F bonds. Therefore, the rate of the C-F bond rupture reaction is also positively influenced by the coverage of C-F bonds in graphene sheets.

Overall, The defluorination of fluorinated graphene is mainly affected by nucleophilicity of solvent, treatment temperature and time, and coverage of C-F bonds. The CxFy composition of treated FG samples can be controlled by adjusting solvent, reaction temperature and time, and it is possible to achieve the complete defluorination of GF to graphene. In addition, the existence of oxygenated groups in the fluorinated graphene sheets may play some roles for its performance. However, this has not been reflected by sufficient information here. More detail studies will be done in future.

4. Conclusions

After treated by some dipolar solvents (NMP, DMF and DMAc), a series of changes took place in the structure and properties of FG even at room temperature, such as a decline of fluorine concentration of about 40 %, the reduction of thermal stability and band gap from 3 to 2 eV, and an improvement of electrochemical performance at high discharge rate. It is supposed that the dipolar solvent interact with the carbon atom of C-F bonds not the fluorine atom via dipolar-dipolar interaction, and releases energy for promoting the rupture of C-F bonds. The rate of reduction of FG is positively influenced by the dipole moment of solvent and fluorine coverage of FG sheets. It is evident that the choosing of solvent is extremely important for the some unique applications of FG. The results will draw more attention to explore the effect of external factors on the physical and chemical characteristics of FG, which is of great importance in order to enhance the performances of FG.

Acknowledgements

This work was supported by the National Natural Science Foundation of China (Grant No.51573105) and financially supported by State Key Laboratory of Polymer Materials Engineering (Grant No. sklpme2014-2-04) andNSERC strategic network Sentinel-Bioactive Paper (Canada). We acknowledge Analytical & Testing Centre Sichuan University, P. R. China for characterization.

Notes and references

1. R. Zboril, F. Karlicky, A. B. Bourlinos, T. A. Steriotis, A. K. Stubos, V. Georgakilas, K. Safařova, D. Jancík, C. Trapalis, M. Otyepka , *Small* 2010, **6**, 2885−2891.
2. R. R. Nair, W. Ren, R. Jalil, I. Riaz, V. G. Kravets, L. Britnell, P. Blake, F. Schedin, A. S. Mayorov and S. Yuan, *Small*, 2010, **6**, 2877-2884.
3. K. Samanta, S. Some, Y. Kim, Y. Yoon, M. Min, S. M. Lee, Y. Park and H. Lee, *Chem Commun*, 2013, **49**, 8991-8993.
4. K. Jeon, Z. Lee, E. Pollak, L. Moreschini, A. Bostwick, C. Park, R. Mendelsberg, V. Radmilovic, R. Kostecki and T. J. Richardson, *ACS nano*, 2011, **5**, 1042-1046.
5. P. Meduri, H. Chen, J. Xiao, J. J. Martinez, T. Carlson, J. Zhang and Z. D. Deng, *J Mater Chem A*, 2013, **1**, 7866-7869.
6. Y. Li, F. Li and Z. Chen, *J Am Chem Soc*, 2012, **134**, 11269-11275.
7. F. Karlický, K. Kumara Ramanatha Datta, M. Otyepka and R. Zbořil, *ACS nano*, 2013, **7**, 6434-6464.
8. Y. Wang, W. C. Lee, K. K. Manga, P. K. Ang, J. Lu, Y. P. Liu, C. T. Lim and K. P. Loh, *Adv Mater*, 2012, **24**, 4285-4290.

9. C. Sun, Y. Feng, Y. Li, C. Qin, Q. Zhang and W. Feng, *Nanoscale*, 2014.

10. J. H. Lee, G. K. W. Koon, D. W. Shin, V. E. Fedorov, J. Y. Choi, J. B. Yoo and B. Özyilmaz, *Adv Funct Mater*, 2013, **23**, 3329-3334.

11. A. K. Geim and K. S. Novoselov, *Nat mater*, 2007, **6**, 183-191.

12. T. Nakajima and H. Groult, *Fluorinated materials for energy conversion*, Elsevier, 2005.

13. X. Wang, Y. Dai, J. Gao, J. Huang, B. Li, C. Fan, J. Yang and X. Liu, *ACS Appl Mater Inter*, 2013, **5**, 8294-8299

14. H. Touhara and F. Okino, *Carbon*, 2000, **38**, 241-267.

15. J. Parmentier, S. Schlienger, M. Dubois, E. Disa, F. Masin and T. A. Centeno, *Carbon*, 2012, **50**, 5135-5147.

16. H. Peng, Z. Gu, J. Yang, J. L. Zimmerman, P. A. Willis, M. J. Bronikowski, R. E. Smalley, R. H. Hauge and J. L. Margrave, *Nano Lett*, 2001, **1**, 625-629.

17. A. Hamwi, *J Phys Chem Solids*, 1996, **57**, 677-688.

18. A. Hamwi, P. Gendraud, H. Gaucher, S. Bonnamy and F. Beguin, *Molecular Crystals and Liquid Crystals*, 1998, **310**, 185-190.

19. R. Yazami, A. Hamwi, K. Guérin, Y. Ozawa, M. Dubois, J. Giraudet and F. Masin, *Electrochem Commun*, 2007, **9**, 1850-1855.

20. M. X. Pulikkathara, O. V. Kuznetsov and V. N. Khabashesku, *Chem Mater*, 2008, **20**, 2685-2695.

21. R. Stine, J. W. Ciszek, D. E. Barlow, W. Lee, J. T. Robinson and P. E. Sheehan, *Langmuir*, 2012, **28**, 7957-7961.

22. V. N. Khabashesku, W. E. Billups and J. L. Margrave, *Accounts Chem Res*, 2002, **35**, 1087-1095.

23. X. Wang, Y. Dai, W. Wang, M. Ren, B. Li, C. Fan and X. Liu, *ACS Appl Mater Inter*, 2014, **6**, 16182-16188.

24. P. Gong, Z. Wang, J. Wang, H. Wang, Z. Li, Z. Fan, Y. Xu, X. Han and S. Yang, *J Mater Chem*, 2012, **22**, 16950-16956.

25. M. Zhu, X. Xie, Y. Guo, P. Chen, X. Ou, G. Yu and M. Liu, *Phys Chem Chem Phys*, 2013, **15**, 20992-21000.

26. J. I. Paredes, S. Villar-Rodil, A. Martinez-Alonso and J. Tascon, *Langmuir*, 2008, **24**, 10560-10564.

27. K. Ai, Y. Liu, L. Lu, X. Cheng and L. Huo, *J Mater Chem*, 2011, **21**, 3365-3370.

28. S. Cheng, K. Zou, F. Okino, H. R. Gutierrez, A. Gupta, N. Shen, P. C. Eklund, J. O. Sofo and J. Zhu, *Phys Rev B*, 2010, **81**, 205435.

29. M. J. McAllister, J. Li, D. H. Adamson, H. C. Schniepp, A. A. Abdala, J. Liu, M. Herrera-Alonso, D. L. Milius, R. Car and R. K. Prud'Homme, *Chem Mater,* 2007, **19**, 4396-4404.

30. C. Gómez-Navarro, J. C. Meyer, R. S. Sundaram, A. Chuvilin, S. Kurasch, M. Burghard, K. Kern and U. Kaiser, *Nano lett* 2010, **10**, 1144-1148.

31. K. Oshida, M. Endo, T. Nakajima, S. L. Di Vittorio, M. S. Dresselhaus and G. Dresselhaus, *J Mater Res*, 1993, **8**, 512-522.

32. Y. M. Shulga, T. Tien, C. Huang, S. Lo, V. E. Muradyan, N. V. Polyakova, Y. Ling, R. O. Loutfy and A. P. Moravsky, *J Electron Spectrosc*, 2007, **160**, 22-28.

33. S. D. Sherpa, S. A. Paniagua, G. Levitin, S. R. Marder, M. D. Williams and D. W. Hess, *J Vac Sci Technol B*, 2012, **30**, 3D-102D.

34. Y. Sato, K. Itoh, R. Hagiwara, T. Fukunaga and Y. Ito, *Carbon*, 2004, **42**, 3243-3249.

35. R. Stine, W. Lee, K. E. Whitener Jr, J. T. Robinson and P. E. Sheehan, *Nano Lett*, 2013, **13**, 4311-4316.

36. H. F. Bettinger, K. N. Kudin and G. E. Scuseria, *J Phys Chem A*, 2004, **108**, 3016-3018.

37. I. P. Asanov, A. V. Okotrub, A. V. Gusel Nikov, I. V. Yushina, D. V. Vyalikh and L. G. Bulusheva, *Carbon*, 2015, **82**, 446-458.

38. V. E. Fedorov, E. D. Grayfer, V. G. Makotchenko, A. S. Nazarov, H. Shin and J. Choi, *Croat Chem Act a*, 2012, **85**, 107-112

39. M. Ren, X. Wang, C. Dong, B. Li, Y. Liu, T. Chen, P. Wu, Z. Cheng, and X. Liu , *Phys Chem Chem Phys*, 2015, **17**, 24056-24062

40. M. Dubecký, E. Otyepková, P. Lazar, F. Karlický, M. Petr, K. Čépe, P. Banáš, R. Zbořil, and Michal Otyepka, *J Phys Chem Lett*, 2015, **6**, 1430-1434.

41. V. Urbanová, K. Holá, A. B. Bourlinos, K. Čépe, A. Ambrosi, A. H. Loo, M. Pumera, F. Karlický, M. Otyepka, and R. Zbořil, *Adv Mater,* 27, 14, 2407-2407.

